SAR of 9-Amino-1,2,3,4-tetrahydroacridine-Based Acetylcholinesterase Inhibitors: Synthesis, Enzyme Inhibitory Activity, QSAR, and Structure-Based CoMFA of Tacrine Analogues

Maurizio Recanatini,* Andrea Cavalli, Federica Belluti, Lorna Piazzi, Angela Rampa, Alessandra Bisi, Silvia Gobbi, Piero Valenti, Vincenza Andrisano, Manuela Bartolini, and Vanni Cavrini

Department of Pharmaceutical Sciences, University of Bologna, Via Belmeloro 6, I-40126 Bologna, Italy

Received December 22, 1999

In this study, we attempted to derive a comprehensive SAR picture for the class of acetylcholinesterase (AChE) inhibitors related to tacrine, a drug currently in use for the treatment of the Alzheimer's disease. To this aim, we synthesized and tested a series of 9-amino-1,2,3,4-tetrahydroacridine derivatives substituted in the positions 6 and 7 of the acridine nucleus and bearing selected groups on the 9-amino function. By means of the Hansch approach, QSAR equations were obtained, quantitatively accounting for both the detrimental steric effect of substituents in position 7 and the favorable electron-attracting effect exerted by substituents in positions 6 and 7 of the 9-amino-1,2,3,4-tetrahydroacridine derivatives. The three-dimensional (3D) properties of the inhibitors were taken into consideration by performing a CoMFA analysis on the series of AChE inhibitors made by 12 9-amino-1,2,3,4-tetrahydroacridines and 13 11*H*-indeno[1,2-*b*]quinolin-10-ylamines previously developed in our laboratory. The alignment of the molecules to be submitted to the CoMFA procedure was carried out by taking advantage of docking models calculated for the interactions of both the unsubstituted 9-amino-1,2,3,4-tetrahydroacridine and 11*H*-indeno[1,2-*b*]quinolin-10-ylamine with the target enzyme. A highly significant CoMFA model was obtained using the steric field alone, and the features of such a 3D QSAR model were compared with the classical QSAR equations previously calculated. The two models appeared consistent, the main aspects they had in common being (a) the individuation of the strongly negative contribution of the substituents in position 7 of tacrine and (b) a tentative assignment of the hydrophobic character to the favorable effect exerted by the substituents in position 6. Finally, a new previously unreported tacrine derivative designed on the basis of both the classical and the 3D QSAR equations was synthesized and kinetically evaluated, to test the predictive ability of the QSAR models. The 6-bromo-9-amino-1,2,3,4-tetrahydroacridine was predicted to have a pIC_{50} value of 7.31 by the classical QSAR model and 7.40 by the CoMFA model, while its experimental IC_{50} value was equal to 0.066 (±0.009) μM, corresponding to a pIC_{50} of 7.18, showing a reasonable agreement between predicted and observed AChE inhibition data.

Introduction

Tacrine (9-amino-1,2,3,4-tetrahydroacridine) is a reversible inhibitor of acetylcholinesterase (AChE) that was launched in 1993 as the first drug for the symptomatic treatment of Alzheimer's disease (AD).[1] The rationale for its use was related to the elevation of the acetylcholine (ACh) levels that can compensate for the cholinergic deficit associated to the brain lesions present in AD. Further outcomes of the so-called "cholinergic hypothesis" are donepezil and rivastigmine, which have been marketed more recently for the treatment of the cognitive symptoms of AD[2] (Chart 1).

Although a number of therapeutic possibilities are emerging aimed at an early intervention on the sequence of neuropathological events leading to the AD dementia,[3] no actual cure is presently available for the disease. On the other hand, recent evaluations of the clinical effects of tacrine have shown efficacy in delaying the deterioration of the symptoms of AD, while confirming the adverse events consisting mainly in the elevated liver transaminase levels and in dose-related peripheral cholinergic effects.[4]

Chart 1. Drugs Presently Marketed for the Treatment of AD

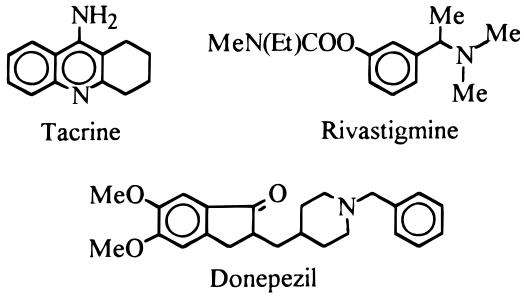

The study of tacrine analogues is still of interest to medicinal chemists involved in AD research. In fact, quite recently, the possibility to design potent and selective bis-tetrahydroaminoacridine inhibitors of AChE was demonstrated,[5] and furthermore, McKenna et al.[6] modified tacrine in such a way as to obtain AChE

* To whom correspondence should be addressed. Tel: +39 051 2099700. Fax: +39 051 2099734. E-mail: mreca@alma.unibo.it.

10.1021/jm990971t CCC: $19.00
Published on Web 04/25/2000

Chart 2. General Structures of the 9-Amino-1,2,3,4-tetrahydroacridine (**I**) and 11*H*-Indeno[1,2-*b*]quinolin-10-ylamine (**II**) Derivatives

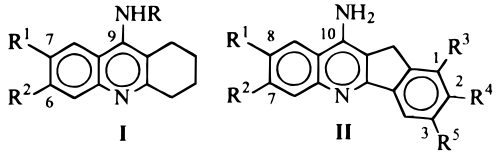

inhibitors able to inhibit 5-HT uptake as well. Despite these achievements, few reports exist in the literature dealing with systematic modification of the tetrahydroaminoacridine nucleus in view of an assessment of the structure−activity relationships (SAR) of this class of compounds.[7−13]

In a recent paper,[14] we performed a comparative QSAR analysis of the main classes of AChE inhibitors under consideration for the use in the treatment of AD: physostigmine derivatives, tetrahydroaminoacridines, and benzylamines. The aim of the work was to individuate the physicochemical properties governing the inhibitory activity of such compounds and to build simple regression models correlating inhibitory potency and properties, to be subsequently used for the design of new inhibitors. As regards the tacrine analogues, we could only determine a dependence of the AChE inhibitory activity on the length of the 9-amino substituent, while almost no indications could be obtained about nuclear substitutions: the reason for this is that very few tetrahydroaminoacridine analogues carrying ring substituents have been synthesized and tested as AChE inhibitors.

To fill the gap in the SAR of tacrine analogues, we decided to carry on our work on 9-amino-1,2,3,4-tetrahydroacridine-based AChE inhibitors[12,15] by synthesizing and testing a series of tacrine derivatives substituted in positions 6 and 7 of the acridine nucleus and bearing selected groups on the 9-amino function (Chart 2, general structure **I**). The biological data (IC_{50} values for the inhibition of isolated human AChE) were then studied by means of the QSAR approach, in search for correlation equations describing the dependence of the AChE inhibitory activity on the physicochemical characteristics of the substituents. Moreover, we attempted to obtain a three-dimensional (3D) quantitative description of the SAR of tetrahydroaminoacridine derivatives using the CoMFA method and including in the series some 11*H*-indeno[1,2-*b*]quinolin-10-ylamine derivatives (Chart 2, general structure **II**) recently developed in our laboratory.[15] The outcome of the present work is a comprehensive qualitative and quantitative description of the interaction of 9-amino-1,2,3,4-tetrahydroacridine-based AChE inhibitors with the enzyme, which completes the picture of the SAR of this class of compounds. The AChE inhibitory activity of a new analogue synthesized for the purpose of testing the QSAR models confirms the theoretical results.

Chemistry

Substituent Selection. The selection of the substituents to be introduced in positions 6 and 7 of the acridine nucleus and on the 9-amino function was dictated by criteria of minimum effort and maximum informative content. Following this line, we chose the smallest number of easily synthetically accessible compounds which could give the maximum spread and orthogonality of the main physicochemical properties, i.e., the hydrophobic, steric, and electronic ones. This lead us to synthesize 11 mono- and disubstituted tacrine derivatives (Table 1), some of which were already known as AChE inhibitors. Notwithstanding this, compounds **1**−**11** plus tacrine provided a set of 12 consistently tested 9-amino-1,2,3,4-tetrahydroacridine derivatives bearing in positions 6 and 7 substituents that display uncorrelated hydrophobic, electronic, and steric properties, as shown by the squared correlation matrix of the descriptors reported in Table 2.

Scheme 1[a]

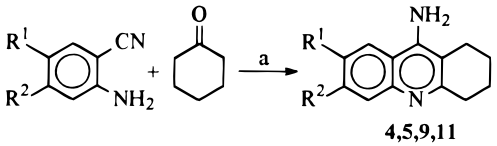

[a] Reagents: (a) $ZnCl_2$, 130 °C, 3 h.

Scheme 2[a]

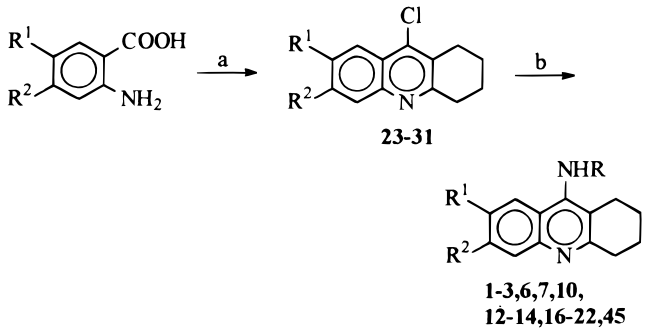

[a] Reagents: (a) cyclohexanone, $POCl_3$, reflux, 2 h; (b) phenol, selected amine, 130 °C, 4 h.

Some of the above derivatives were further modified by inserting a substituent on the 9-NH_2 group (compounds **12**−**22**, Table 1). Such a modification was introduced in the 6- or 7-substituted analogues showing the best anticholinesterase activity within the set. As the R groups, the benzyl and *n*-heptyl ones were selected, which had already been tested as substituents in the corresponding position of tacrine analogues by us[15] and also by others.[7,8,11]

Synthetic Methods. The substituted 9-amino-1,2,3,4-tetrahydroacridines reported in Table 1 (general structure **I**, Chart 2) were prepared by conventional synthetic methods. No attempt was made to improve the reaction yields.

In Scheme 1, the synthesis of compounds **4**, **5**, **9**, and **11** is illustrated. These compounds were prepared by condensation of selected 2-aminobenzonitriles (anthranilonitriles) with cyclohexanone in the presence of $ZnCl_2$. Compound **8** was obtained by reduction of **5** with Fe/HCl, while treatment of **5** with benzyl bromide in the presence of tetrabutylammonium hydrogen sulfate gave compound **15**.

Compounds **1**−**3**, **6**, **7**, **10**, **12**−**14**, **16**−**22**, and **45** were prepared as shown in Scheme 2. By heating the selected anthranilic acid and cyclohexanone, the 9-chloro-1,2,3,4-terahydroacridines **23**−**31** were obtained, which were treated with ammonia, benzylamine, or heptylamine to yield the desired compounds.

Table 1. Structural Data and AChE Inhibitory Activity (IC_{50}) of the 9-Amino-1,2,3,4-tetrahydroacridine Derivatives

no.	R	R^1	R^2	formula	yield, %	mp, °C	$IC_{50} \pm SE$, μM
1[a]	H	CH_3	H	$C_{14}H_{16}N_2$	20	223−225	8.1 ± 0.6
2	H	H	CH_3	$C_{14}H_{16}N_2$	30	220−222	0.10 ± 0.01
3	H	Cl	H	$C_{13}H_{13}ClN_2$	50	254−256[b]	0.55 ± 0.02
4	H	H	Cl	$C_{13}H_{13}ClN_2$	50	296−298[c]	0.0099 ± 0.0003
5	H	NO_2	H	$C_{13}H_{13}N_3O_2$	50	264−266[d]	3.0 ± 0.2
6	H	H	NO_2	$C_{13}H_{13}N_3O_2$	20	260−262	0.028 ± 0.001
7	H	H	OCH_3	$C_{14}H_{16}N_2O$	50	181−183[e]	0.35 ± 0.01
8[f]	H	NH_2	H	$C_{13}H_{15}N_3$	60	118−120	3.8 ± 0.2
9[f]	H	H	F	$C_{13}H_{13}FN_2$	30	210−212	0.087 ± 0.001
10	H	Cl	Cl	$C_{13}H_{12}Cl_2N_2$	20	265−267	0.47 ± 0.02
11	H	OCH_3	OCH_3	$C_{15}H_{18}N_2O_2$	30	275−277[g]	5.2 ± 0.1
12	$CH_2C_6H_5$	CH_3	H	$C_{21}H_{22}N_2$	60	120−122	3.7 ± 0.2
13	$CH_2C_6H_5$	H	CH_3	$C_{21}H_{22}N_2$	50	245−247	0.75 ± 0.03
14	$CH_2C_6H_5$	H	Cl	$C_{20}H_{19}ClN_2$	20	>300 dec	0.17 ± 0.01
15	$CH_2C_6H_5$	NO_2	H	$C_{20}H_{19}N_3O_2$	50	184−186	1.6 ± 0.1
16	$CH_2C_6H_5$	H	NO_2	$C_{20}H_{19}N_3O_2$	30	166−168	4.8 ± 0.4
17	C_7H_{15}	CH_3	H	$C_{21}H_{30}N_2$	30	48−50	0.39 ± 0.03
18	C_7H_{15}	H	CH_3	$C_{21}H_{30}N_2$	50	49−51	0.13 ± 0.01
19	C_7H_{15}	H	Cl	$C_{20}H_{27}ClN_2$	40	80−82	0.013 ± 0.004
20	C_7H_{15}	H	NO_2	$C_{20}H_{23}N_3O_2$	20	66−68	0.29 ± 0.02
21	C_7H_{15}	H	OCH_3	$C_{21}H_{30}N_2O$	40	84−86[h]	0.46 ± 0.01
22	C_7H_{15}	H	F	$C_{20}H_{27}FN_2$	40	219−221	0.045 ± 0.002
tacrine	H	H	H				0.25 ± 0.01

[a] Ref 16. [b] Lit.[9] mp > 230 °C dec. [c] Lit.[9] mp 262−264 °C dec. [d] Lit.[10] mp 197−198 °C. [e] Lit.[11] mp 213-214 °C. [f] Ref 17. [g] Lit.[11] mp 237−239 °C. [h] Lit.[11] mp 92−94 °C.

The synthesis of the 11*H*-indeno[1,2-*b*]quinolin-10-ylamine derivatives of Table 4 (general structure **II**, Chart 2) is reported in ref 15. Not commercially available substituted anthranilonitriles and anthranilic acids were prepared from the corresponding anilines by the isatin route.

Results

The inhibitory activity against human erythrocyte AChE of 6-, 7-, and N9-substituted derivatives of the 9-amino-1,2,3,4-tetrahydroacridine and of the reference compound tacrine is reported in Table 1, expressed as IC_{50} values. For all the compounds studied, the inhibition of AChE activity was very fast, not time-dependent (the 50% enzyme inactivation produced by the IC_{50} concentrations following a 1-min incubation was not significantly ($P > 0.01$) different from the inhibition observed up to a 40-min incubation) and reversible.

SAR. It is evident that both the nature and the position on the ring of the 6- and 7-substituents are able to vary the biological activity of the unsubstituted parent compound (tacrine). For example, it was already known[9] that the chlorine atom in the 6-position strongly increases the inhibitory potency of tacrine, while the 7-chloro analogue does not (compounds **4** and **3**, respectively). We found a similar effect for both the CH_3 (compounds **2** and **1**) and the NO_2 groups (compounds **6** and **5**). Other substituents modify only slightly the inhibitory activity of tacrine, like 6-OCH_3 (compound **7**), or decrease it, like 7-NH_2 (compound **8**), or increase it, like 6-F (compound **9**). As regards the double substitution, in the case of the 6,7-dichloro derivative, it appears that the favorable effect of Cl in position 6 is canceled by the presence of the second chlorine atom (compound **10**). The same seems to hold for the monomethoxy (compound **7**) and dimethoxy (compounds **11**) derivatives, as already reported by Del Giudice et al.[11]

The introduction of substituents on the 9-NH_2 function of the tetrahydroacridine nucleus was limited to the benzyl and *n*-heptyl groups, as they can provide a substantial increase of lipophilicity while showing different steric characteristics. Moreover, we already studied the effects of these substituents in a related series of 11*H*-indeno[1,2-*b*]quinolin-10-ylamines.[15] In the present work, we partially confirmed those results, as we found that the benzyl group decreases the AChE inhibitory effect for the 6-substituted tetrahydroacridine analogues (compounds **13**, **14**, **16**) and for the 7-CH_3 analogue (compound **12**), while it causes a slight increase for the 7-NO_2-substituted derivative (compound **15**). As regards the *n*-heptyl group, it strongly increases the activity of the 7-methyl analogue (compound **17**) and leaves almost unchanged the inhibitory potency of the remaining 6-substituted compounds (compounds **18**−**22**).

The qualitative SAR picture that emerges from the above results can be summarized in a few points: (a) substituents in position 6 of the 9-amino-1,2,3,4-tetrahydroacridine nucleus exert more favorable effects on the AChE inhibitory activity than substituents in position 7; (b) the 6,7-disubstitution cancels the favorable effect of the 6-substituent; (c) a benzyl group on the 9-amino function generally leads to a lower inhibitory potency, while a *n*-heptyl one does not have a substantial effect. Of course, the above points are tentative generalizations that can be contradicted by some single case (e.g., compound **17**).

QSAR. With the aim to rationalize in terms of physicochemical properties the SAR of tacrine derivatives, we applied to the series of compounds under study the classical Hansch analysis, looking for correlations between the variation of inhibitory activity and the variation of parameters describing the hydrophobic, electronic, and steric properties of the molecules.[18] As stated in the Introduction, the substituents in positions 6 and 7 were selected in such a way as to provide an acceptable compromise between the maximum spread of each property and the orthogonality of the variables (see Table 2). The parameters used in this study and

Table 2. Squared Correlation Matrix of the Parameters Used in the QSAR Analysis

	$\pi(R^1)$	$\pi(R^2)$	$MR(R^1)$	$MR(R^2)$	$F(R^1,R^2)$	$R(R^1,R^2)$
$\pi(R^1)$		0.057	0.005	0.015	0.074	0.066
$\pi(R^2)$			0.019	0.049	0.010	0.000
$MR(R^1)$				0.045	0.106	0.116
$MR(R^2)$					0.141	0.091
$F(R^1,R^2)$						0.000
$R(R^1,R^2)$						

from which the squared correlation matrix of Table 2 was calculated are the substituent constants π, *MR*, *F*, and *R*, describing the hydrophobic, steric, and electronic (field and resonance) characteristics of the substituents, respectively. The π and *MR* values were assigned to substituents in each of the 6- and 7-positions, while to describe the electronic effects also in the case of disubstituted derivatives, the sum of the *F* and *R* values for the two positions was used for all the compounds. Due to the limited variation of the substituents on the 9-NH_2 function, we introduced two indicator variables, *I-B* and *I-H*, to take into account the presence of the benzyl or *n*-heptyl group, respectively. The complete list of the parameters used to derive the correlation equations is shown in Table 3, together with the activity data transformed into pIC_{50} values.

As the first step in the derivation of a meaningful QSAR model for tacrine analogues, we tried to calculate a correlation equation based on all the compounds of the series, and obtained eq 3 as the best significant correlation for the 23 compounds. The stepwise development of eq 3 is the following:

$$pIC_{50} = -2.06(\pm1.05)MR(R^1) + 7.05(\pm0.43) \quad (1)$$

$$n = 23\ r^2 = 0.444\ s = 0.639\ F_{1,21(\text{total})} = 16.76$$

$$pIC_{50} = -1.82(\pm0.99)MR(R^1) + 0.84(\pm0.78)\pi(R^2) + 6.83(\pm0.44) \quad (2)$$

$$n = 23\ r^2 = 0.555\ s = 0.586\ F_{2,20(\text{total})} = 12.48 \qquad F_{1,20(\text{partial})} = 5.01$$

$$pIC_{50} = -1.78(\pm0.88)MR(R^1) + 0.88(\pm0.70)\pi(R^2) - 0.67(\pm0.55)I\text{-}B + 6.96(\pm0.41) \quad (3)$$

$$n = 23\ r^2 = 0.668\ s = 0.519\ F_{3,19(\text{total})} = 12.73 \qquad F_{1,19(\text{partial})} = 6.45$$

In the above equations and in all the other ones in this paper, *n* is the number of data points from which the equation was calculated, r^2 is the correlation coefficient, and *s* is the standard deviation of the regression; $F_{(\text{total})}$ and $F_{(\text{partial})}$ are the values of the Fisher's test for the overall significance of the equation and for the introduction of the last variable, respectively.

Equation 3, which is the best one obtainable from the data at hand, is actually a poor correlation equation explaining only about the 67% of the variance of the AChE inhibition data. Moreover, the introduction of the last variable, *I-B*, the indicator variable for the presence of the benzyl group on the N9 atom, is significant only at the $\alpha > 0.05$ level, as it is the introduction of the $\pi(R^2)$ term in eq 2. These statistics point out some weakness of the model, which, on the other hand, is rather stable throughout the stepwise derivation, with regard to the regression coefficients associated to the $MR(R^1)$ and $\pi(R^2)$ variables.

From eq 3, one can obtain a first indication that the variation of the pIC_{50} data is affected at least partly by the steric properties (unfavorable) of the substituents in position 7 and by the hydrophobic characteristics (favorable) of the substituents in position 6; the benzyl group in position N9 contributes negatively to the activity by decreasing the pIC_{50} values of about 0.7 log unit. Finally, eq 3 cannot be used for predictive purposes.

In an attempt to pursue a more precise description of the effects of substituents in the critical 6- and 7-positions of the tetrahydroacridine nucleus, we decided to study only the N9-unsubstituted compounds **1**−**11** (plus tacrine). This was done considering that the conformational flexibility of both the benzyl and *n*-heptyl groups could make it questionable the choice of proper physicochemical parameters for the 9-substituents. The most significant equation obtained from the 12 data points is eq 5, which contains the electronic term $F(R^1,R^2)$ together with the $MR(R^1)$ term present also in eq 3:

$$pIC_{50} = -2.63(\pm1.31)MR(R^1) + 7.35(\pm0.60) \quad (4)$$

$$n = 12\ r^2 = 0.668\ s = 0.560\ F_{1,10(\text{total})} = 20.09$$

$$pIC_{50} = -3.09(\pm1.03)MR(R^1) + 1.43(\pm0.99)F(R^1,R^2) + 7.00(\pm0.50) \quad (5)$$

$$n = 12\ r^2 = 0.847\ s = 0.400\ F_{2,9(\text{total})} = 24.88 \qquad F_{1,9(\text{partial})} = 10.52\ q^2_{\text{loo}} = 0.769$$

Equation 5, although showing a rather high standard deviation, can be considered as a statistically acceptable QSAR model; the introduction of the electronic parameter $F(R^1,R^2)$ can be regarded as significant at an $\alpha > 0.01$ level, the critical $F_{1,9}$ value being equal to 10.56. For eq 5, we calculated also the cross-validated regression coefficient by using the leave-one-out technique (q^2_{loo}); considering its good value, one can be rather confident in the predictive power of the QSAR.

In eq 5, the most important term is again the $MR(R^1)$ parameter that confirms the detrimental effect of 7-substituents on the AChE inhibitory activity. However, when the N9-substituted derivatives are excluded, the inductive (field) electronic effect of the 6- and 7-substituents comes into light: it seems that the former substituents increase the inhibitory activity of the compounds by exerting an electron-attracting action (positive coefficient) on the tetrahydroacridine nucleus. There is no hydrophobic term in eq 3, which might mean that the property is not important or, otherwise, that the series is not wide and/or varied enough to allow that effect to be detected.

The picture emerging from eq 5 regards only the effects of the substituents in positions 6 and 7 and it shows a negative steric influence on the AChE inhibitory activity carried out by groups in position 7 and a favorable electron-attracting effect exerted by the substituents on the ring.

Table 3. Activity Data and Parameters Used for Derivation of the QSAR Eqs 1−5

no.	pIC_{50}	$\pi(R^1)$	$\pi(R^2)$	$MR(R^1)$	$MR(R^2)$	$F(R^1,R^2)$	$R(R^1,R^2)$	*I-B*	*I-H*
1	5.09	0.560	0.000	0.565	0.103	0.010	−0.180	0	0
2	7.00	0.000	0.560	0.103	0.565	0.010	−0.180	0	0
3	6.26	0.710	0.000	0.603	0.103	0.420	−0.190	0	0
4	8.00	0.000	0.710	0.103	0.603	0.420	−0.190	0	0
5	5.52	−0.280	0.000	0.736	0.103	0.650	0.130	0	0
6	7.55	0.000	−0.280	0.103	0.736	0.650	0.130	0	0
7	6.45	0.000	−0.020	0.103	0.787	0.290	−0.560	0	0
8	5.42	−1.230	0.000	0.542	0.103	0.080	−0.740	0	0
9	7.06	0.000	0.140	0.103	0.092	0.450	−0.390	0	0
10	6.32	0.710	0.710	0.603	0.603	0.840	−0.380	0	0
11	5.29	−0.020	−0.020	0.787	0.787	0.580	−1.120	0	0
12	5.43	0.560	0.000	0.565	0.103	0.010	−0.180	1	0
13	6.13	0.000	0.560	0.103	0.565	0.010	−0.180	1	0
14	6.77	0.000	0.710	0.103	0.603	0.420	−0.190	1	0
15	5.80	−0.280	0.000	0.736	0.103	0.650	0.130	1	0
16	5.32	0.000	−0.280	0.103	0.736	0.650	0.130	1	0
17	6.41	0.560	0.000	0.565	0.103	0.010	−0.180	0	1
18	6.89	0.000	0.560	0.103	0.565	0.010	−0.180	0	1
19	7.88	0.000	0.710	0.103	0.603	0.420	−0.190	0	1
20	6.53	0.000	−0.280	0.103	0.736	0.650	0.130	0	1
21	6.33	0.000	−0.020	0.103	0.787	0.290	−0.560	0	1
22	7.34	0.000	0.140	0.103	0.092	0.450	−0.390	0	1
tacrine	6.59	0.000	0.000	0.103	0.103	0.000	0.000	0	0

Table 4. Structure of the 11*H*-Indeno[1,2-*b*]quinolin-10-ylamine Derivatives[a] Used in the CoMFA Analysis

no.	R^1	R^2	R^3	R^4	R^5
32	H	H	H	H	H
33	NH_2	H	H	H	H
34	H	NO_2	H	H	H
35	H	NH_2	H	H	H
36	H	Cl	H	H	H
37	H	F	H	H	H
38	H	H	OCH_3	H	H
39	H	H	H	OCH_3	H
40	H	H	H	H	OCH_3
41	H	H	CH_3	H	H
42	H	H	H	H	CH_3
43	H	H	H	F	H
44	H	H	H	Cl	H

[a] Ref 15.

3D QSAR. A further step toward both the definition and the illustration of the SAR of tacrine analogues was the consideration of the 3D properties of the compounds. This was initially accomplished by using the comparative molecular field analysis (CoMFA)[19] method that allowed us to derive a 3D QSAR model for AChE inhibitors based on the 9-amino-1,2,3,4-tetrahydroacridine nucleus.

To carry out the analysis, we again decided to study only the 6- and 7-substituted compounds and to exclude the N9-substituted derivatives for the reason outlined above; that is because the conformational flexibility of both the benzyl and *n*-heptyl groups could render it difficult and perhaps meaningless the individuation of one putative active conformation. However, to extend the database on which to perform the 3D analysis, we added to the tetrahydroacridine set a series of 11*H*-indeno[1,2-*b*]quinolin-10-ylamine derivatives that was recently developed and published by us[15] (Chart 2, general structure **II**; Table 4). These compounds can be considered as tacrine derivatives bearing substituents in positions corresponding to the tacrine's 6 and 7 and expanding the polycyclic nucleus through the replacement of the tetrahydrophenyl moiety with an indenyl one. By means of kinetic experiments, we have been able to show that the indenoquinoline derivatives not substituted on the 10-amino function display the same mode of AChE inhibition as tacrine, i.e., a mixed type inhibition.

The mutual alignment of the molecules to be submitted to the CoMFA procedure, which is the critical step of the analysis,[20] was carried out by taking advantage of docking models developed for the interaction of tacrine and of the parent unsubstituted 11*H*-indeno[1,2-*b*]quinolin-10-ylamine **32**. Based on the X-ray coordinates of the tacrine−AChE complex[21] and suitably modifying the structure of the ligand, a starting model of the indenoquinoline−AChE complex was built. After the appropriate minimization and molecular dynamics simulation steps, we could obtain a docking model showing the interactions between **32** and some critical residues of the AChE active site gorge.[15] The same computational protocol was applied to the tacrine−AChE complex for consistency, and after superimposition of the AChE backbone atoms of the two models, the ligands tacrine and **32** were extracted, each maintaining the orientation it assumes in the enzyme active site. In Figure 1, the mutual orientation of the two parent molecules is shown as it resulted from the docking experiments. The alignment of the molecules for the CoMFA analysis was then obtained by superimposing each analogue on the respective template, i.e., compounds **1**−**11** on tacrine and compounds **33**−**44** on **32**.

To obtain the 3D QSAR equations, PLS analyses were performed using each of the steric and electrostatic CoMFA fields alone and also, as usual, in combination. The results of the analyses are shown in Table 5, from which it is possible to see that the use of the steric field only gave the best statistical result. Model 1 was thus chosen as the working CoMFA model, whose descriptivity and predictivity are assessed by the r^2 value of 0.817 and q^2 value of 0.669, respectively. As in the QSAR model (eq 5), the standard deviation is rather high, in both the cross-validated (s_{cross}) and non-cross-validated (s) cases.

The results of the comparative molecular field analysis can be illustrated by plotting the isocontour maps calculated from the QSAR equation expressing the non-

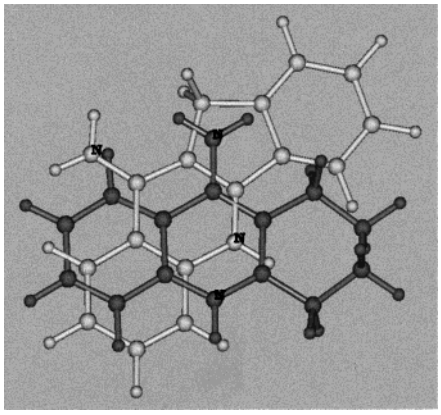

Figure 1. Superimposition of the unsubstituted 9-amino-1,2,3,4-tetrahydroacridine (gray) and 11*H*-indeno[1,2-*b*]quinolin-10-ylamine (white) resulting from the fitting of the enzymes' backbone atoms of the AChE−tacrine and AChE−**32** complexes, respectively.

Table 5. Summary of the CoMFA Results and Statistics

	model 1 (steric field)	model 2 (electrostatic field)	model 3 (steric and electrostatic fields)
q^2	0.669	0.178	0.653
s_{cross}	0.549	0.845	0.561
r^2	0.817	0.788	0.829
s	0.407	0.485	0.394
n	25	25	25
F	49.18	11.16	53.20
optimal no. of components	2	1	2

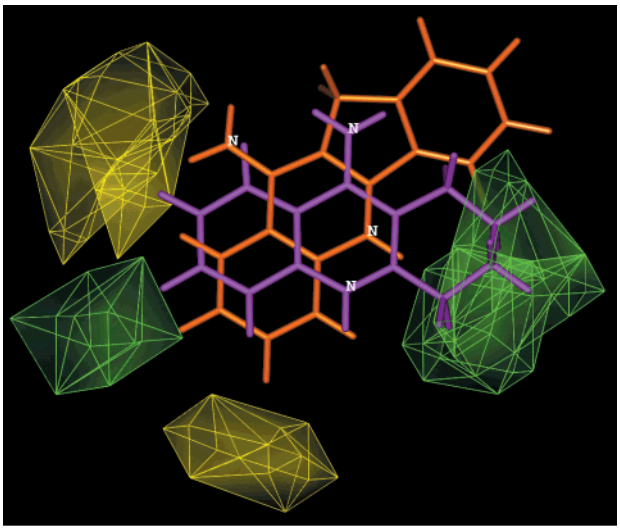

Figure 2. View of the steric CoMFA STDEV*COEFF contour maps (model 1, Table 5). The region where increasing the volume increases activity is green (0.020 level), and the region where increasing the volume decreases activity is yellow (−0.040 level). The parent compounds 9-amino-1,2,3,4-tetrahydroacridine (magenta) and 11*H*-indeno[1,2-*b*]quinolin-10-ylamine (orange) are shown for reference.

cross-validated model. The isocontours generated by interpolating the STDEV*COEFF terms of the conventional CoMFA equation for the steric contribution are shown in Figure 2. CoMFA contour plots are shown surrounding regions in the space around the templates tacrine (magenta) and **32** (orange), where the steric properties of the molecules influence the AChE inhibitory activity. The steric contours are colored green where addition of steric bulk increases the activity and yellow where an increase of the inhibitor's volume causes a decrease of activity.

Considering the position of the isocontours in the space around the reference molecules, it can be observed that part of the steric effects significative for the variation of the anticholinesterase activity of the series arise from the variation of the substituents located on the quinolinic benzene of the molecules. In particular, a green favorable contour (Figure 2, left) is located in a position corresponding mostly to the 6-substituents of tacrine and partly to the 8-substituents of **32**. The yellow unfavorable steric contours are mainly located over the 7-position of tacrine (Figure 2, top left) covering an area that comprises also the NH_2 function of the indenoquinoline analogues and partly corresponding to the 7-position of **32** (Figure 2, bottom). Another relevant favorable green volume surrounds the 2-, 3-, and 4-positions of the tacrine derivatives (Figure 2, right) indicating the higher activity of that subset of analogues.

The picture shown in Figure 2, if considered in all its components (reference molecules and contours), summarizes on a statistical basis the 3D SAR for the two series of tacrine analogues. In fact, it shows how the prototype molecules are mutually oriented in order to bind to the same enzyme active site, and it also shows which zones of the space around the overlapped molecules are available or forbidden for a (steric) modification. The most interesting feature of the CoMFA model is the individuation of the narrow sterically favorable "window" embedded between two sterically unfavorable zones and corresponding to the position occupied by the 6-substituents of tacrine.

To get an objective validation of the two quantitative models developed to describe the SAR of tetrahydroacridine-based AChE inhibitors, we synthesized a new tacrine analogue whose experimentally determined activity was compared with that predicted by both models. The previously unreported 6-bromo-9-amino-1,2,3,4-tetrahydroacridine (**45**) was predicted to have a pIC_{50} value of 7.31 by the QSAR model (eq 5) and 7.40 by the CoMFA model (steric field only). The experimental IC_{50} value was 0.066 (±0.009) μM, corresponding to a pIC_{50} of 7.18. It may be concluded that the activity values calculated by the QSAR and 3D QSAR models are in reasonable agreement with the observed value, despite the fact that the QSAR equation uses a steric and an electronic parameter, while the CoMFA equation uses only the steric field. Interestingly, the QSAR model approaches the real value slightly more closely.

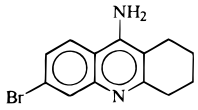

45

Discussion

Since the paper of Steinberg et al. on noncovalent AChE inhibitors related to 9-amino-1,2,3,4-tetrahydroacridine,[7] only few articles have been published dealing with structural modifications of tacrine[8−13,15] or with bis-tetrahydroacridine derivatives.[5] In our comparative QSAR paper published in 1997,[14] we pointed

out the lack of comprehensive SAR work on the tacrine-related class of inhibitors of AChE and indicated the need to synthesize and test a set of carefully designed analogues able to provide a sound basis for a QSAR study. In this paper, we present such a group of compounds and derive a SAR picture by taking advantage of a number of computational techniques. Actually, it seemed to us that the QSAR approach could be more suitable than a traditional SAR study for both rationalizing and summarizing the effects of structural variations of the molecules on the anticholinesterase activity. Consequently, here we will discuss essentially the QSAR and 3D QSAR results regarding the nuclear modifications brought on the 9-amino-1,2,3,4-tetrahydroacridine parent structure.

As regards the QSAR analysis, the model to be taken into consideration is that expressed by eq 5, and it would not be the case to discuss eq 3, unless one noticed that it contains the indicator variable *I-B* (accounting for the presence of the benzyl group on the 9-amino group) with a negative coefficient. It might be observed that the appearance of this slightly negative effect exerted by the 9-*N*-benzyl substituent is in agreement with the findings of Steinberg et al.[7] and Shutske et al.,[8] who studied the effects of amino substituents on 9-aminotetrahydroacridine and 9-aminotetrahydroacridin-1-ol derivatives, respectively.

The common motif throughout eqs 1−5 is the presence of the term $MR(R^1)$ bearing a negative coefficient. This indicates a negative steric effect carried out by any substituent in position 7 of tacrine, also reported by other authors.[8,9,11] Interestingly, in the most statistically significant eq 5, the presence of an electronic term ($F(R^1,R^2)$, positive coefficient) indicates favorable electron-attracting effects caused by both the 6- and 7-substituents. The role of electron-attracting electronic effects on the interaction of 6-chlorotacrine with AChE was pointed out by Wlodek et al.,[22] who, on the basis of theoretical calculations, gave a tentative explanation of such effects, suggesting that the reduced electron density on the tacrine aromatic rings could favor π-electron interactions with nearby residues, like Phe330 and Trp84.

A number of CoMFA models have already been published on AChE inhibitors,[23−26] but none deals exclusively with 9-amino-1,2,3,4-tetrahydroacridine-related compounds. In three cases,[24−26] the authors performed a structure-based alignment of the molecules to be analyzed, which was allowed by the availability of the crystal structures of AChE−inhibitor complexes. We followed the procedure indicated by Cho et al.,[24] fitting the coordinates of the crystallographically resolved AChE−tacrine complex and those of the modeled AChE−11*H*-indeno[1,2-*b*]quinolin-10-ylamine complex. The resulting superimposition of the two prototype inhibitors shown in Figure 1 was used as the template for the alignment of the respective derivatives. It is worth noting that a CoMFA analysis performed on the same series of molecules aligned by superimposing the atoms of the aminoquinoline moieties common to the two subsets gave an unacceptably low q^2 value (data not shown). Notably, this was a case where a structure-based alignment lead to better results than a simple "objective" atom-by-atom superimposition of the common structural features of the molecules.

Table 6. Experimental pIC_{50} Values for Inhibition of AChE, Predicted pIC_{50} Values from the QSAR and CoMFA Models, and Deviations from Experimental Values

		QSAR		CoMFA	
no.	pIC_{50} (exptl)	pIC_{50} (calcd)	deviat	pIC_{50} (calcd)	deviat
1	5.09	5.27	−0.18	5.09	0.00
2	7.00	6.70	0.30	7.31	−0.31
3	6.26	5.74	0.52	5.79	0.47
4	8.00	7.29	0.71	7.45	0.55
5	5.52	5.66	−0.14	5.70	−0.18
6	7.55	7.61	−0.06	7.34	0.21
7	6.45	7.10	−0.65	6.76	−0.31
8	5.42	5.44	−0.02	5.85	−0.43
9	7.06	7.33	−0.27	7.05	0.01
10	6.32	6.34	−0.02	6.28	0.04
11	5.29	5.40	−0.11	5.01	0.28
32	6.17			5.53	0.64
33	5.23			5.82	−0.59
34	4.17			4.69	−0.52
35	4.54			4.89	−0.35
36	5.18			4.90	0.28
37	5.92			5.30	0.62
38	5.78			5.81	−0.03
39	5.19			5.45	−0.25
40	5.37			5.46	−0.09
41	5.41			5.65	−0.24
42	5.34			5.40	−0.06
43	6.36			5.54	0.82
44	5.27			5.44	−0.17
tacrine	6.59	6.68	−0.09	6.98	−0.39

The reported CoMFA model is highly significant from a statistical point of view (Table 5), even if one calculated pIC_{50} value deviates from the corresponding experimental one by about twice the standard deviation (Table 6, compound **43**, deviation CoMFA = 0.82). The anticholinesterase activity of **43** is strongly underpredicted, as are, even if at a lesser extent, the activity values of **32** (deviation CoMFA = 0.64) and **37** (deviation CoMFA = 0.62). These sensible differences between the calculated and observed pIC_{50} values and, in general, the rather high standard deviation of the CoMFA equation might be a consequence of the alignment strategy, which is structure-based for the two prototypes but atom-by-atom for their substituted analogues. This might lead to neglecting some subtle aspect of the enzyme−inhibitor docking, and it is likely to increase the uncertainty in the estimate of the activity. Actually, Bernard et al.,[26] studying a set of AChE inhibitors, found better CoMFA results when each of the training set molecules was individually docked into the enzyme active site. However, the deviations of the F-substituted compounds **37** and **43** might also be due to the fact that only the steric field was used in the derivation of the model. It is reasonable to hypothesize that the steric characteristics of the fluorine atom are not relevant enough to account for the observed variations of pIC_{50}.

Another feature of the CoMFA model deserving a comment is the need of the steric field only to obtain a statistically satisfactory model. It appears from the statistics reported in Table 5 that the electrostatic field did not contribute to the explanation of the variance of the activity data, such that it was not included in the derivation of the PLS model. In the previously published CoMFA analyses concerning AChE inhibitors, the results regarding the relative field contributions are

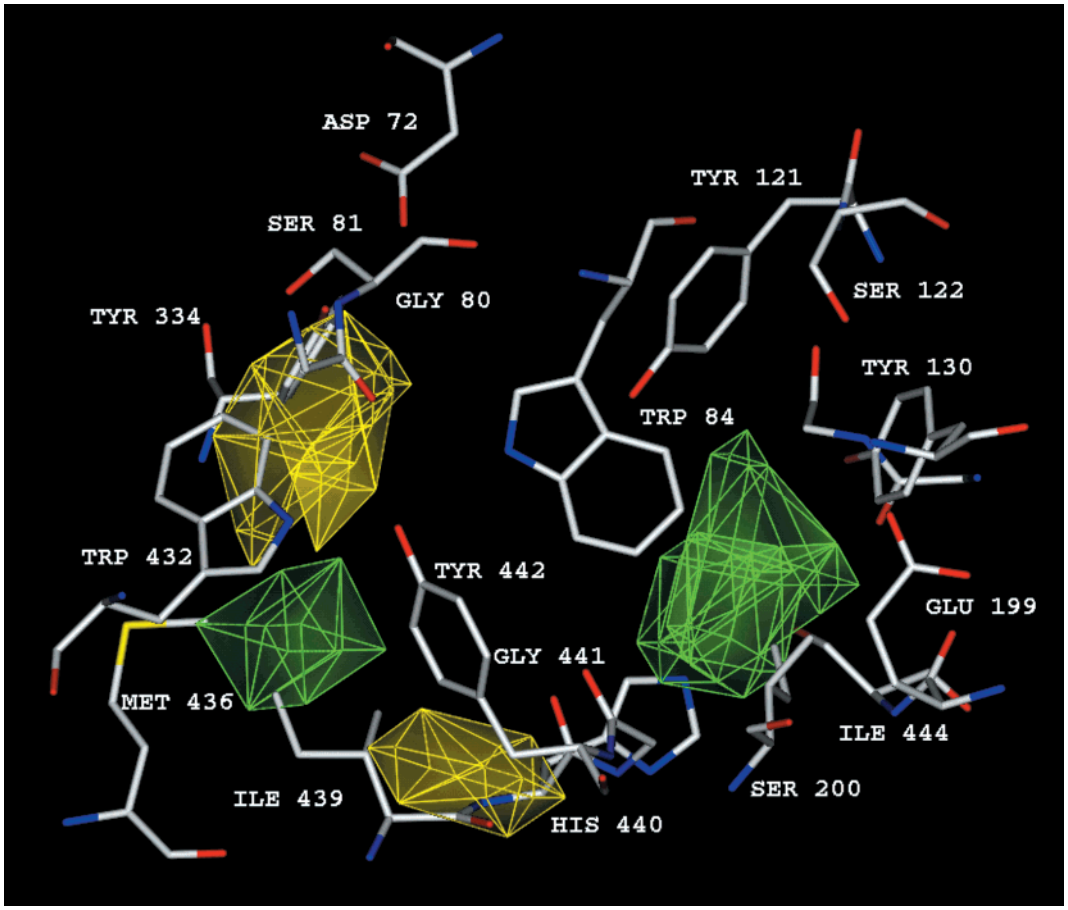

Figure 3. Superimposition of the steric CoMFA contour plots and some active site residues of AChE.

different, as it is reasonably expected considering the structural differences of the training sets. In the model of Bernard et al.,[26] there is a prevalence of the electrostatic field contribution (66.8% electrostatic, 33.2% steric), while in the model developed by Cho et al.,[24] the steric field contributes more, in both the conventional and q^2-GRS analyses. However, it is interesting to note that Tong et al.,[23] who studied the molecules (benzylpiperidine derivatives) in both the neutral and protonated states, found a definitely greater steric field contribution (73.5% steric, 26.5% electrostatic) when the molecules were considered in the protonated form. We modeled the molecules in the protonated state, as it is supposed that 4-aminoquinoline-related derivatives are ionized on the ring nitrogen atom at the pH of the biological experiment.[7] As may be inferred by the finding of Tong et al.,[23] it is possible that the formal positive charge carried by the molecules obscures the electronic effects exerted by the substituents and levels off the electrostatic field values that, accordingly, are not varied enough to provide a significant contribute in the PLS analysis.

The QSAR and 3D QSAR models can be compared, to assess their consistency in describing the SAR of the AChE inhibitors studied in the present paper. As outlined above, the most reliable QSAR model is represented by eq 5, which deals with 12 tacrine analogues (Table 1, compounds **1**−**11** plus tacrine); the features of the CoMFA model obtained from the 25 compounds of Table 6 (tetrahydroacridines and indenoquinolines) are shown in Figure 2. The most relevant aspect the two models have in common is the individuation of the strongly negative steric contribution of the substituents in position 7 of the tacrine nucleus. The yellow area top left of Figure 2 is perfectly consistent with the negative $MR(R^1)$ term of eq 5. Of course, there is no possibility to interpret the electronic term $F(R^1,R^2)$ of the QSAR equation with reference to the CoMFA model, whereas the hydrophobic $\pi(R^2)$ term present in eqs 2 and 3 could tentatively be viewed as a possible explanation of the sterically favorable green zone left in Figure 2. The extreme caution required in considering the poorly significant eqs 2 and 3 needs however to be stressed.

To put the ligand-based QSAR and CoMFA models in a perspective that takes into consideration the structure of the target enzyme,[27] we examined the position of the CoMFA contours in the AChE active site. This is a common practice when the 3D structure of the target protein is available, and actually, it has been done in two of the above-cited CoMFA studies on AChE inhibitors.[24,25] Even if the CoMFA contour maps can by no means be interpreted as some sort of 3D "complementary" picture of an enzyme active site, it is reasonable to look for some consistency of the steric (and, eventually, electrostatic) features revealed by the 3D statistical analysis and the "actual" enzyme−ligand interaction site. In Figure 3, the CoMFA contour plots are overlapped onto the part of the AChE active site structure where the tacrine analogues bind, and it appears that a satisfactory concordance exists between the statistical and the graphic models. In fact, the yellow sterically forbidden areas of the CoMFA model overlay on some amino acid residues. In particular, the yellow bottom zone engulfs some backbone atoms of Ile439 and

His440, and the other yellow area occupies the space around some backbone atoms of Ser81 and the side chains of Tyr334 and Trp432. On the contrary, the green sterically favorable volume on the right of the picture fills an empty volume of the enzyme active site. Remarkably, the left green zone occupies an area where the side chains of Met436 and Ile439 fall, and this observation is intriguing, because it again leads to the hypothesis that the positive steric interaction in this zone can be interpreted as the possibility of a favorable hydrophobic contact between the substituents in position 6 of the tetrahydroacridine-derived inhibitors and the mentioned residues. At the light of this hypothesis, the presence of the $\pi(R^2)$ term in eqs 2 and 3 might not be exclusively seen as a mere statistical artifact.

Conclusions

In this study, we attempted to derive a comprehensive SAR picture able to summarize the effects of the introduction of substituents in some position of tacrine, the lead compound of a class of noncovalent AChE inhibitors. To achieve the goal, we synthesized and tested a number of substituted analogues that constitute a set of structurally varied compounds to be analyzed by means of the QSAR approach. Moreover, with the aim to obtain a 3D description of the QSAR of the class, we extended the training set of AChE inhibitors by adding to the tetrahydroacridines a set of recently developed indenoquinoline derivatives. The QSAR and CoMFA analyses provided two separate models that show a satisfactory consistency, pointing out two main SAR aspects of the tetrahydroacridine-based AChE inhibitors: (a) the negative steric effect of substituents in position 7 and (b) the relative steric freedom of position 6. The comparison of the two quantitative models with a 3D picture of the AChE active site derived from the X-ray resolved structure supported those conclusions and allowed to hypothesize the possibility of a hydrophobic interaction between some enzyme residues and substituents in position 6 of tacrine. The kinetic evaluation of the AChE inhibitory activity of a new tacrine derivative designed on the basis of both the classical and 3D QSAR equations and purposely synthesized allowed us to assess the good predictivity of the models and to confirm the reliability of the SAR conclusions.

It can be concluded that, for an important class of AChE inhibitors, the proper selection of a small set of compounds and the application of QSAR techniques in conjunction with a 3D model of the target protein lead to a formulation of the SAR suitable for both descriptive and predictive purposes.

Experimental Section

Chemistry. General Methods. All melting points were determined in open glass capillaries using a Büchi apparatus and are uncorrected. ^{1}H NMR spectra were recorded in $CDCl_3$ solution on a Varian Gemini 300 spectrometer with Me_4Si as the internal standard. Wherever analyses are only indicated with elements symbols, analytical results obtained for those elements are within 0.4% of the theoretical values.

Preparation of Compounds 4, 5, 9, and 11. A mixture of selected anthranilonitrile (0.01 mol), cyclohexanone (0.01 mol) and dry $ZnCl_2$ (3 g) was heated at 120−130 °C for 3 h. After cooling, the reaction mixture was treated with water and the separated solid, collected by filtration, was crystallized from suitable solvent or purified by flash chromatography (silica gel 60, Merck, Darmstadt, Germany; ethyl acetate/methanol 9/1).

^{1}H NMR ($CDCl_3$) and Mass Spectra for Compounds 4, 5, 9, and 11. 4: δ 1.70−1.76 (m, 2H), 2.32−2.41 (m, 2H), 2.70−2.80 (m, 4H), 5.21 (br, 2H, NH_2), 7.03−7.73 (m, 3H, Ar); MS *m*/*z* (relative abundance) 232 (M^+, 100), 216 (10.9), 204 (11.0). Anal. ($C_{13}H_{13}ClN_2$) C, H, N. **5**: δ 1.85−2.02 (m, 4H), 2.58−2.68 (m, 2H), 3.02−3.12 (m, 2H), 4.98 (br, 2H, NH_2), 7.95−8.83 (m, 3H, Ar); MS *m*/*z* (relative abundance) 243 (M^+, 100), 196 (16.7), 91 (11.4). Anal. ($C_{13}H_{13}N_3O_2$) C, H, N. **9**: δ 1.82−1.88 (m, 4H), 2.48−2.58 (m, 2H), 2.88−2.95 (m, 2H), 4.89 (br, 2H, NH_2), 7.01−7.79 (m, 3H, Ar); MS *m*/*z* (relative abundance) 216 (M^+, 90.4), 91 (65.0), 32 (100). Anal. ($C_{13}H_{13}FN_2$) C, H, N. **11**: δ 1.73−1.89 (m, 4H), 2.47−2.54 (m, 2H), 2.82−2.92 (m, 2H), 3.92 (s, 6H), 7.22 (s, 1H, Ar), 7.81 (s, 1H, Ar); MS *m*/*z* (relative abundance) 258 (M^+, 100), 243 (25.0), 215 (11.0). Anal. ($C_{15}H_{18}N_2O_2$) C, H, N.

7,9-Diamino-1,2,3,4-tetrahydroacridine (8). A solution of **5** (1.2 g, 5 mmol) in ethanol (50 mL) and HCl (1.5 mL) was refluxed and Fe (1.8 g) was added portionwise in 2 h. The reaction mixture was refluxed 2 h and hot filtered. The solvent was evaporated at reduced pressure and the residue was taken up in water, treated with solid $NaHCO_3$ and extracted with CH_2Cl_2. The solution was dried and evaporated to dryness to yield a solid which was crystallized from ethanol to give 0.63 g (60%) of **8**: mp 181−183 °C; ^{1}H NMR δ 1.74−1.87 (m, 4H), 2.43−2.56 (m, 2H), 2.78−2.84 (m, 2H), 5.32 (br, 2H, NH_2), 6.89 (br, 2H, NH_2), 7.09−7.53 (m, 3H, Ar); MS *m*/*z* (relative abundance) 213 (M^+, 100), 197 (11.9), 185 (9.9). Anal. ($C_{13}H_{15}N_3$) C, H, N.

7-Nitro-9-benzylamino-1,2,3,4-tetrahydroacridine (15). A solution of **5** (1.2 g, 5 mmol) in CH_2Cl_2 (100 mL) was treated with 50% NaOH solution, tetrabutylammonium hydrogen sulfate (1.7 g, 5 mol) and benzyl bromide (0.86 g, 5 mmol) and the reaction mixture was stirred at room temperature for 4 h. The organic layer was separated, washed with water, dried and evaporated to dryness. The residue, purified by flash chromatography (toluene−ethyl acetate 4/1), yielded 0.83 g (50%) of **15:** mp 184−186 °C (toluene); ^{1}H NMR δ 1.87−1.98 (m, 4H), 2.58−2.62 (m, 2H), 3.05−3.11 (m, 2H), 4.62 (br, 1H, NH), 4.84 (s, 2H), 7.32−9.09 (m, 8H, Ar); MS *m*/*z* (relative abundance) 333 (M^+, 70.8), 242 (10.0), 91 (100). Anal. ($C_{20}H_{19}N_3O_2$) C, H, N.

General Method for the Preparation of Substituted 9-Chloro-1,2,3,4-tetrahydroacridines 23−31. A mixture of selected anthranilic acid (0.01 mol), cyclohexanone (0.01 mol) in $POCl_3$ (10 mL) was refluxed for 2 h. The reaction mixture was evaporated and treated with ice and $NaHCO_3$ solid. The separated solid was taken up in ether. The solution was washed with water, dried and evaporated. The residue was purified by crystallization from petroleum ether or by flash chromatography to give the desired compounds.

7-Methyl-9-chloro-1,2,3,4-tetrahydroacridine (23): purified by flash chromatography, yield 60%; mp 77−79 °C (ligroin); ^{1}H NMR δ 1.82−2.02 (m, 4H), 2.53 (s, 3H), 2.92−3.12 (m, 4H), 7.43−7.93 (m, 3H, Ar). Anal. ($C_{14}H_{14}ClN$) C, H, N.

6-Methyl-9-chloro-1,2,3,4-tetrahydroacridine (24): purified by flash chromatography, yield 70%; mp 80−82 °C (ligroin); ^{1}H NMR δ 1.88−2.0 (m, 4H), 2.55 (s, 3H), 2.96−3.07 (m, 2H), 3.08−3.15 (m, 2H), 7.32−8.07 (m, 3H, Ar). Anal. ($C_{14}H_{14}ClN$) C, H, N.

7,9-Dichloro-1,2,3,4-tetrahydroacridine (25): yield 65%; mp 120−122 °C (ligroin); ^{1}H NMR δ 1.81−2.02 (m, 4H), 2.98−3.16 (m, 4H), 7.57−8.20 (m, 3H, Ar). Anal. ($C_{13}H_{11}Cl_2N$) C, H, N.

6,9-Dichloro-1,2,3,4-tetrahydroacridine (26): purified by flash chromatography, yield 60%; mp 77−79 °C (ligroin); ^{1}H NMR δ 1.78−1.98 (m, 4H), 2.81−3.12 (m, 4H), 7.07−8.0 (m, 3H, Ar). Anal. ($C_{13}H_{11}Cl_2N$) C, H, N.

6-Nitro-9-chloro-1,2,3,4-tetrahydroacridine (27): yield 50%; mp 150−152 °C (ligroin); ^{1}H NMR δ 1.91−2.07 (m, 4H),

3.02−3.19 (m, 4H), 8.31−8.32 (m, 2H, Ar), 8.90 (s, 1H, Ar). Anal. ($C_{13}H_{11}ClN_2O_2$) C, H, N.

6-Methoxy-9-chloro-1,2,3,4-tetrahydroacridine (28): purified by flash chromatography, yield 55%; mp 90−92 °C (ligroin); ^{1}H NMR δ 1.80−1.99 (m, 4H), 2.85−3.09 (m, 4H), 3.88 (s, 3H), 7.07−8.03 (m, 3H, Ar). Anal. ($C_{14}H_{14}ClNO$) C, H, N.

6-Fluoro-9-chloro-1,2,3,4-tetrahydroacridine (29): yield 65%; mp 75−77 °C (ligroin); ^{1}H NMR δ 1.89−2.0 (m, 4H), 2.93−3.14 (m, 4H), 7.29−8.23 (m, 3H, Ar). Anal. ($C_{13}H_{11}ClFN$) C, H, N.

6-Bromo-9-chloro-1,2,3,4-tetrahydroacridine (30): yield 60%; mp 73−74 °C (ligroin); ^{1}H NMR δ 1.90−2.01 (m, 4H), 2.94−3.18 (m, 4H), 7.35−8.01 (m, 3H, Ar). Anal. ($C_{13}H_{11}BrClN$) C, H, N.

6,7,9-Trichloro-1,2,3,4-tetrahydroacridine (31): yield 60%; oil; ^{1}H NMR δ 1.83−2.01 (m, 4H), 2.91−3.12 (m, 4H), 8.14 (s, 1H, Ar), 8.23 (s, 1H, Ar). Anal. ($C_{13}H_{10}Cl_3N$) C, H, N.

Preparation of Compounds 1−3, 6, 7, 10, and 45. A mixture of selected 9-chloro-1,2,3,4-tetrahydroacridine (3.5 mmol) in phenol (3.12 g) was heated at 85−90 °C until an homogeneous solution was obtained. The mixture was heated at 125−130 °C for 4 h while a stream of NH_3(g) was bubbled. After cooling, ethyl acetate was added and the obtained solution was treated with 10% NaOH solution, water and dried. The solvent was removed under reduced pressure and the residue was purified by flash chromatography (silica gel 60, Merck, Darmstadt, Germany; ethyl acetate/methanol 9/1).

^{1}H NMR ($CDCl_3$) and Mass Spectra for Compounds 1−3, 6, 7, 10, and 45. 1: δ 1.78−1.88 (m, 4H), 1.38 (s, 3H), 2.74−2.88 (m, 2H), 3.02−3.12 (m, 2H), 4.96 (br, 2H, NH_2), 7.17−7.68 (m, 3H, Ar); MS *m*/*z* (relative abundance) 212 (M^+, 10.1), 77 (51.4), 57 (100). Anal. ($C_{14}H_{16}N_2$) C, H, N. **2**: δ 1.63−1.73 (m, 2H), 2.26 (s, 3H), 2.35−2.39 (m, 2H), 2.62−2.72 (m, 4H), 5.0 (br, 2H, NH_2), 6.88−7.57 (m, 3H, Ar); MS *m*/*z* (relative abundance) 212 (M^+, 22.1), 149 (49.0), 57 (100). Anal. ($C_{14}H_{16}N_2$) C, H, N. **3**: δ 1.65−1.85 (m, 4H), 2.35−2.43 (m, 2H), 2.75−2.83 (m, 2H), 5.14 (br, 2H, NH_2), 7.25−7.81 (m, 3H, Ar); MS *m*/*z* (relative abundance) 232 (M^+, 100), 92 (17.4), 63 (60.2). Anal. ($C_{13}H_{13}ClN_2$) C, H, N. **6**: δ 1.86−1.95 (m, 4H), 2.51−2.60 (m, 2H), 2.91−3.03 (m, 2H), 5.70 (br, 2H, NH_2), 7.89−8.73 (m, 3H, Ar); MS *m*/*z* (relative abundance) 243 (M^+, 100), 215 (6.9), 197 (18.9). Anal. ($C_{13}H_{13}N_3O_2$) C, H, N. **7**: δ 1.82−2.01 (m, 4H), 2.50−2.61 (m, 2H), 2.92−3.02 (m, 2H), 3.91 (s, 3H), 4.75 (br, 2H, NH_2), 6.95−7.62 (m, 3H, Ar); MS *m*/*z* (relative abundance) 228 (M^+, 2.9), 94 (100), 66 (48.0). Anal. ($C_{14}H_{16}N_2O$) C, H, N. **10**: δ 1.91−2.08 (m, 4H), 2.55−2.68 (m, 2H), 2.98−3.08 (m, 2H), 4.66 (br, 2H, NH_2), 7.79 (s, 1H, Ar), 8.01 (s, 1H, Ar); MS *m*/*z* (relative abundance) 266 (M^+, 100), 250 (11.4), 238 (12.9). Anal. ($C_{13}H_{12}Cl_2N_2$) C, H, N. **45**: δ 1.85−2.01 (m, 4H), 2.48−2.59 (m, 2H), 2.97−3.01 (m, 2H), 5.93 (br, 2H, NH_2), 7.29−7.91 (m, 3H, Ar); MS *m*/*z* (relative abundance) 276 (M^+, 100), 232 (17.1), 195 (11.3). Anal. ($C_{13}H_{13}BrN_2$) C, H, N.

Preparation of Compounds 12−14 and 16−22. A mixture of selected 9-chloro-1,2,3,4-tetrahydroacridine (3.5 mmol) in phenol (3.12 g) was heated at 85−90 °C until an homogeneous solution was obtained. Heptylamine or benzylamine (7.7 mmol) was added and the mixture was heated at 125−130 °C for 4 h. After cooling ethyl acetate was added and the obtained solution was treated with 10% NaOH solution, water and dried. The solvent was removed under reduced pressure and the residue was purified by flash chromatography (silica gel 60, Merck, Darmstadt, Germany; ethyl acetate/methanol 9.5/0.5).

^{1}H NMR ($CDCl_3$) and Mass Spectra for Compounds 12−14 and 16−22. 12: δ 1.72−1.93 (m, 4H), 2.48 (s, 3H), 2.55−2.65 (m, 2H), 2.99−3.07 (m, 2H), 4.02 (br, 1H, NH), 4.57 (s, 2H), 7.25−7.88 (m, 8H, Ar); MS *m*/*z* (relative abundance) 302 (M^+, 21.0), 218 (33.4), 91 (100). Anal. ($C_{21}H_{22}N_2$) C, H, N. **13**: δ 1.85−1.98 (m, 4H), 2.52 (s, 3H), 2.62−2.66 (m, 2H), 3.03−3.09 (m, 2H), 4.15 (br, 1H, NH), 4.62 (d, 2H), 7.18−7.92 (m, 8H, Ar); MS *m*/*z* (relative abundance) 302 (M^+, 13.4), 211 (29.0), 91 (100). Anal. ($C_{21}H_{22}N_2$) C, H, N. **14**: δ 1.82−1.95 (m, 4H), 2.58−2.63 (m, 2H), 3.02−3.06 (m, 2H), 4.2 (br, 1H, NH), 4.63 (s, 2H), 7.28−7.97 (m, 8H, Ar); MS *m*/*z* (relative abundance) 322 (M^+, 3.1), 232 (30.3), 91 (100). Anal. ($C_{20}H_{19}ClN_2$) C, H, N. **16**: δ 1.85−1.94 (m, 4H), 2.57−2.78 (m, 2H), 3.03−3.14 (m, 2H), 4.65 (s, 2H), 7.35−8.83 (m, 8H, Ar); MS *m*/*z* (relative abundance) 333 (M^+, 14.6), 304 (6.7), 91 (100). Anal. ($C_{20}H_{19}N_3O_2$) C, H, N. **17**: δ 0.85−0.97 (m, 3H), 1.22−1.43 (m, 8H), 1.62−1.77 (m, 2H), 1.85−1.97 (m, 4H), 2.52 (s, 3H), 2.68−2.73 (m, 2H), 3.03−3.07 (m, 2H), 3.46−3.51 (t, 2H), 7.38−7.88 (m, 3H, Ar); MS *m*/*z* (relative abundance) 310 (M^+, 58.0), 225 (100), 211 (21.1). Anal. ($C_{21}H_{30}N_2$) C, H, N. **18**: δ 0.88−0.94 (m, 3H), 1.20−1.35 (m, 8H), 1.92−1.98 (m, 4H), 2.25 (s, 3H), 2.58−2.70 (m, 2H), 3.09−3.19 (m, 2H), 3.47−3.54 (t, 2H), 7.13−7.90 (m, 3H, Ar); MS *m*/*z* (relative abundance) 310 (M^+, 48.3), 225 (100), 211 (31.2). Anal. ($C_{21}H_{30}N_2$) C, H, N. **19**: δ 0.73−0.93 (m, 3H), 1.12−1.48 (m, 8H), 1.52−1.78 (m, 2H), 1.82−1.98 (m, 4H), 2.53−2.70 (m, 2H), 2.98−3.03 (m, 2H), 3.91 (br, 1H, NH), 7.30−7.95 (m, 3H, Ar); MS *m*/*z* (relative abundance) 330 (M^+, 56.2), 245 (100), 231 (21.9). Anal. ($C_{20}H_{27}ClN_2$) C, H, N. **20**: δ 0.86−0.92 (m, 3H), 1.21−1.47 (m, 8H), 1.61−1.74 (m, 2H), 1.89−2.01 (m, 4H), 2.66−2.73 (m, 2H), 3.01−3.11 (m, 2H), 3.47−3.64 (m, 2H), 8.03−8.80 (m, 3H, Ar); MS *m*/*z* (relative abundance) 341 (M^+, 48.5), 242 (53.6), 225 (100). Anal. ($C_{20}H_{23}N_3O_2$) C, H, N. **21**: δ 0.83−0.97 (m, 3H), 1.15−1.38 (m, 8H), 1.57−1.70 (m, 2H), 1.83−2.03 (m, 4H), 2.60−2.70 (m, 2H), 2.98−3.04 (m, 2H), 3.40−3.57 (t, 2H), 3.91 (s, 3H), 6.94−7.90 (m, 3H, Ar); MS *m*/*z* (relative abundance) 326 (M^+, 100), 241 (71.6), 227 (26.5). Anal. ($C_{21}H_{30}N_2O$) C, H, N. **22**: δ 0.75−0.97 (m, 3H), 1.14−1.42 (m, 8H), 1.81−1.99 (m, 4H), 2.54−2.62 (m, 2H), 2.92−3.07 (m, 2H), 4.51 (br, 1H, NH), 7.29−7.98 (m, 2H, Ar); MS *m*/*z* (relative abundance) 314 (M^+, 51.6), 229 (100), 215 (16.5). Anal. ($C_{20}H_{27}FN_2$) C, H, N.

Inhibition of AChE. The method of Ellman et al.[28] was followed. The assay solution consisted of a 0.1 M phosphate buffer, pH 8.0, with the addition of 340 μM 5,5′-dithiobis(2-nitrobenzoic acid) (Ellman's reagent), 0.035 unit/mL AChE derived from human erythrocytes, and 550 μM acetylthiocholine iodide. The final assay volume was 1 mL. Test compounds were added to the assay solution and preincubated with the enzyme for 20 min, the addition of substrate following. Five different concentrations of each inhibitor were used, to obtain inhibition of AChE activity comprised between 20% and 80%.

Initial rate assays were performed at 37 °C with a Jasco V-350 double-beam spectrophotometer: the rate of increase of the absorbance at 412 nm was followed for 5 min. Assays were done with a blank containing all components except AChE, to account for nonenzymatic reaction. The reaction rates were compared and the percent inhibition due to the presence of test compounds was calculated. Each concentration was analyzed in triplicate. The percent inhibition of the enzyme activity due to the presence of increasing test compound concentration was calculated by the following expression: $100 - V_i/V_0 \times 100$, where V_i is the rate calculated in the presence of inhibitor and V_0 is the enzyme activity. Inhibition curves were obtained for each compound by plotting the percent (%) inhibition vs the logarithm of inhibitor concentration in the assay solution. The linear regression parameters were determined for each curve and the IC_{50} values extrapolated.

Acetylthiocholine iodide, 5,5′-dithiobis(2-nitrobenzoic acid), and AChE (0.5 IU/mg) derived from human erythrocytes were purchased from Sigma Chemical. Tacrine (9-amino-1,2,3,4-tetrahydroacridine hydrochloride) was obtained from Aldrich Italia. Buffer components and other chemicals were of the highest purity commercially available.

QSAR and Molecular Modeling. The QSAR analysis was performed by applying the classical Hansch approach and using the C-QSAR program[29] both to retrieve the substituent constants and to calculate the regression equations.

The modeling of the inhibitors and the CoMFA procedures were carried out by means of the SYBYL molecular modeling package.[30] Small molecule models were built by assembling

fragments from the program standard library and energy-optimized by means of the MOPAC AM1 method;[31] partial atomic charges for all the compounds were also calculated using AM1.

The structure-based alignment of the parent compounds tacrine and **32** was obtained by fitting the backbones of the AChE−tacrine and AChE−**32** complexes and then extracting the two inhibitors from the enzyme active sites. The modeling procedure of the AChE−**32** complex, performed using the united-atom AMBER* force field implemented in the MacroModel Ver. 5.5 program,[32] is reported in detail elsewhere[15,33] and only summarized here. Briefly, the coordinates of the AChE−tacrine complex obtained from the X-ray structure determined using AChE from *T. californica* were retrieved from the Brookhaven Protein Data Bank (entry 1acj), and the residue Phe330 was replaced by Tyr, to reproduce the human AChE active site sequence. The inhibitor **32** was built by properly modifying the structure of tacrine and docked into the enzyme active site in the N10-protonated form. All the ionizable residues of the enzyme were kept in the ionized state, and the water molecules present in the PDB file were also maintained in their original positions. The AChE−inhibitor complex was submitted to a molecular modeling protocol aimed at refining the position of **32** in the active site pocket. Minimizations and molecular dynamics (MD) simulations were carried out on a core of unconstrained atoms around the active site (8 Å) and on a shell of constrained atoms (energy penalty force constant of 100 kJ/Å^2 mol^{-1}) surrounding the core (6 Å). An initial minimization (2000 steps, steepest descent) and a subsequent temperature constant MD simulation (140 ps, 298 K, 1.0-fs time step) were carried out. An equilibration time of 60 ps was allowed before starting the data collection. The MD average structure of the last 80 ps was energy-minimized first by steepest descent (3000 steps) and then by conjugate gradient with a derivative convergence criterion of 0.05 kJ/Å^2 mol^{-1}. The same MD protocol was applied to the AChE−tacrine complex, to ensure the consistency of the docking models.

The CoMFA fields were generated using an sp^3 C atom with a +1 charge as the probe, the region was created automatically, and the default grid spacing was used (2 Å). The statistical analysis was performed by applying the PLS procedure to the appropriate columns of the CoMFA table and using the standard scaling method (COMFA_STD). Also, to reduce the actual number of column considered, energy cutoff values of 30 kcal/mol were selected for both electrostatic and steric fields and the minimum σ value was set to 2.0. Cross-validated PLS runs were carried out for establishing the optimum number of components to be used in the final fitting models. The number of cross-validation groups was always equal to the number of compounds (leave-one-out technique), and the optimum number of components was chosen by considering the lowest standard error of prediction (s_{cross}).

Acknowledgment. This investigation was supported by the University of Bologna (funds for selected research topics) and by MURST.

References

(1) Davis, K. L.; Powchik, P. Tacrine. *Lancet* **1995**, *345*, 625−630.
(2) (a) Bartus, R. T.; Dean, L. D. III; Beer, B.; Lippa, A. S. The Cholinergic Hypothesis of Geriatric Memory Dysfunction. *Science* **1982**, *217*, 408−417. (b) Siddiqui, M. F.; Levey, A.-I. Cholinergic Therapies in Alzheimer's Disease. *Drugs Future* **1999**, *24*, 417−424.
(3) Selkoe, D. J. Translating Cell Biology into Therapeutic Advances in Alzheimer's Disease. *Nature* **1999**, *399*, A23−A31.
(4) Gracon, S. I.; Berghoff, W. G. Cholinesterase Inhibition in the Treatment of Alzheimer's Disease: Further Evaluation of the Clinical Effects of Tacrine. In *Pharmacological Treatment of Alzheimer's Disease. Molecular and Neurobiological Foundations*; Brioni, J. D., Decker, M. W, Eds.; Wiley-Liss, Inc.: New York, 1997; pp 389−408.
(5) (a) Pang, Y.-P.; Quiram, P.; Jelacic, T.; Hong, F.; Brimijoin, S. Highly Potent, Selective, and Low Cost Bis-tetrahydroaminacrine Inhibitors of Acetylcholinesterase. *J. Biol. Chem.* **1996**, *271*, 23646−23649. (b) Carlier, P. R.; Han, Y. F.; Chow, E. S.-H.; Li, C. P.-L.; Wang, H.; Lieu, T. X.; Wong, H. S.; Pang, Y.-P. Evaluation of Short-tether Bis-THA AChE Inhibitors. A Further Test of the Dual Binding Site Hypothesis. *Bioorg. Med. Chem.* **1999**, *7*, 351−357. (c) Carlier, P. R.; Chow, E. S.-H.; Han, Y. F.; Liu, J.; El Yazal, J.; Pang, Y.-P. Heterodimeric Tacrine-Based Acetylcholinesterase Inhibitors: Investigating Ligand-Peripheral Site Interactions. *J. Med. Chem.* **1999**, *42*, 4225−4231.
(6) McKenna, M.; Proctor, G. R.; Young, L. C.; Harvey, A. L. Novel Tacrine Analogues for Potential Use against Alzheimer's Disease: Potent and Selective Acetylcholinesterase Inhibitors and 5-HT Uptake Inhibitors. *J. Med. Chem.* **1997**, *40*, 3516−3523.
(7) Steinberg, G. M.; Mednick, M. L.; Maddox, J.; Rice, R. A Hydrophobic Binding Site in Acetylcholinesterase. *J. Med. Chem.* **1975**, *18*, 1056−1061.
(8) Shutske, G. M.; Pierrat, F. A.; Kapples, K. J.; Cornfeldt, M. L.; Szewczac, M. R.; Huger, F. P.; Bores, G. M.; Haroutunian, V.; Davis, K. L. 9-Amino-1,2,3,4-tetrahydroacridin-1-ols: Synthesis and Evaluation as Potential Alzheimer's Disease Therapeutics. *J. Med. Chem.* **1989**, *32*, 1805−1813.
(9) Gregor, V. E.; Emmerling, M. R.; Lee, C.; Moore, C. J. The Synthesis and In Vitro Acetylcholinesterase and Butyrylcholinesterase Inhibitory Activity of Tacrine (Cognex) Derivatives. *Bioorg. Med. Chem. Lett.* **1992**, *2*, 861−864.
(10) Pirrung, M. C.; Chau, J. H.-L.; Chen, J. Discovery of a Novel Tetrahydroacridine Acetylcholinesterase Inhibitor through an Indexed Combinatorial Library. *Chem. Biol.* **1995**, *2*, 621−626.
(11) Del Giudice, M. R.; Borioni, A.; Mustazza, C.; Gatta, F.; Meneguz, A.; Volpe, M. T. Synthesis and Cholinesterase Inhibitory Activity of 6-, 7-Methoxy- (and Hydroxy-) Tacrine Derivatives. *Farmaco* **1996**, *51*, 693−698.
(12) Valenti, P.; Rampa, A.; Bisi, A.; Andrisano, V.; Cavrini, V.; Fin, L.; Buriani, A.; Giusti, P. Acetylcholinesterase Inhibition by Tacrine Analogues. *Bioorg. Med. Chem. Lett.* **1997**, *7*, 2599−2602.
(13) Camps, P.; El Achab, R.; Görbig, D. M.; Morral, J.; Muñoz-Torrero, D.; Badia, A.; Baños, J. E.; Vivas, N. M.; Barril, X.; Orozco, M.; Luque, F. J. Synthesis, In Vitro Pharmacology, and Molecular Modeling of Very Potent Tacrine-Huperzine A Hybrids as Acetylcholinesterase Inhibitors of Potential Interest for the Treatment of Alzheimer's Disease. *J. Med. Chem.* **1999**, *42*, 3227−3242.
(14) Recanatini, M.; Cavalli, A.; Hansch, C. A Comparative QSAR Analysis of Acetylcholinesterase Inhibitors Currently Studied for the Treatment of Alzheimer's Disease. *Chem.-Biol. Interact.* **1997**, *105*, 199−228.
(15) Rampa, A.; Bisi, A.; Belluti, F.; Gobbi, S.; Valenti, P.; Andrisano, V.; Cavrini, V.; Cavalli, A.; Recanatini, M. Acetylcholinesterase Inhibitors for Potential Use in Alzheimer's Disease: Molecular Modeling, Synthesis and Kinetic Evaluation of 11*H*-Indeno-[1,2-b]-quinolin-10-ylamine Derivatives. *Bioorg. Med. Chem.* **2000**, *8*, 497−506.
(16) Bielavsky, J. Single step preparation of 9-amino-1,2,3,4-tetrahydroacridines. Czech. Patent 181,474, 1980; *Chem. Abstr. 93*, 204471j.
(17) Kawakami, H.; Ohuchi, R.; Kitano, M.; Ono, K. Quinoline derivatives. Eur. Patent 268871, 1988; *Chem. Abstr. 109*, 110275v.
(18) Hansch, C.; Leo, A. *Exploring QSAR. Fundamentals and Applications in Chemistry and Biology*; ACS Professional Reference Books; American Chemical Society: Washington, 1995.
(19) Cramer, R. D. III; Patterson, D. E.; Bunce, J. D. Comparative Molecular Field Analysis (CoMFA). 1. Effect of Shape on Binding of Steroids to Carrier Proteins. *J. Am. Chem. Soc.* **1988**, *110*, 5959−5967.
(20) Cramer, R. D. III; DePriest, S. A.; Patterson, D. E.; Hecht, P. The Developing Practice of Comparative Molecular Field Analysis. In *3D QSAR in Drug Design. Theory, Method and Applications*; Kubinyi, H., Ed.; ESCOM: Leiden, 1993; pp 443−485.
(21) Sussman, J. L.; Harel, M.; Silman, I. Three-Dimensional Structure of Acetylcholinesterase and of its Complexes with Anticholinesterase Drugs. *Chem.-Biol. Interact.* **1993**, *87*, 187−197.
(22) Wlodek, S. T.; Antosiewicz, J.; McCammon, J. A.; Straatsma, T. P.; Gilson, M. K.; Briggs, J. M.; Humblet, C.; Sussman, J. L. Binding of Tacrine and 6-Chlorotacrine by Acetylcholinesterase. *Biopolymers* **1996**, *38*, 109−117.
(23) Tong, W.; Collantes, E. R.; Chen, Y.; Welsh, W. J. A Comparative Molecular Field Analysis Study of *N*-Benzylpiperidines as Acetylcholinesterase Inhibitors. *J. Med. Chem.* **1996**, *39*, 380−387.
(24) Cho, S. J.; Serrano Garsia, M. L.; Bier, J.; Tropsha, A. Structure-Based Alignment and Comparative Molecular Field Analysis of Acetylcholinesterase Inhibitors. *J. Med. Chem.* **1996**, *39*, 5064−5071.

(25) Hasegawa, K.; Kimura, T.; Funatsu, K. GA Strategy for Variable Selection in QSAR Studies: Application of GA-Based Region Selection to a 3D-QSAR Study of Acetylcholinesterase Inhibitors. *J. Chem. Inf. Comput. Sci.* **1999**, *39*, 112−120.
(26) Bernard, P.; Kireev, D. B.; Chrétien, J. R.; Fortier, P.-L.; Coppet, L. Automated Docking of 82 *N*-Benzylpiperidine Derivatives to Mouse Acetylcholinesterase and Comparative Molecular Field Analysis with "Natural" Alignment. *J. Comput.-Aided Mol. Des.* **1999**, *13*, 355−371.
(27) Kim, K. H. Building a Bridge Between G-Protein-Coupled Receptor Modelling, Protein Crystallography and 3D QSAR Studies for Ligand Design. In *3D QSAR in Drug Design: Recent Advances*; Kubinyi, H., Folkers, G., Martin, Y. C., Eds.; KLUVER/ESCOM: London, 1998; pp 233−255.
(28) Ellman, G. L.; Courtney, K. D.; Andres, V.; Featherstone, R. M. A New and Rapid Colorimetric Determination of Acetylcholinesterase Activity. *Biochem. Pharmacol.* **1961**, *7*, 88−95.
(29) C-QSAR, ver. 1.87; BioByte: Claremont, CA, 1994.
(30) SYBYL, ver. 6.5; Tripos Associates: St. Louis, MO, 1998.
(31) Dewar, M. J.; Zoebisch, E. G.; Healy, E. F.; Stewart, J. J. P. AM1: a New General Purpose Quantum Mechanical Molecular Model. *J. Am. Chem. Soc.* **1985**, *107*, 3902−3909.
(32) Mohamadi, F.; Richards, N. G. J.; Guida, W. C.; Liskamp, R. M. J.; Lipton, M. A.; Caulfield, C. E.; Chang, G.; Hendrickson, T. F.; Still, W. C. MacroModel − an Integrated Software System for Modeling Organic and Bioorganic Molecules Using Molecular Mechanics. *J. Comput. Chem.* **1990**, *11*, 440−467.
(33) Rampa, A.; Bisi, A.; Valenti, P.; Recanatini, M.; Cavalli, A.; Andrisano, V.; Cavrini, V.; Fin, L.; Buriani, A.; Giusti, P. Acetylcholinesterase Inhibitors: Synthesis and Structure−Activity Relationships of *ω*-[*N*-Methyl-*N*-(3-alkylcarbamoyloxyphenyl)methyl]aminoalkoxyheteroaryl Derivatives. *J. Med. Chem.* **1998**, *41*, 3976−3986.

JM990971T